Journal of Biomechanics 114 (2021) 110160

Contents lists available at ScienceDirect

Journal of Biomechanics

journal homepage: www.elsevier.com/locate/jbiomech
www.JBiomech.com

An individualized linear model approach for estimating scapular kinematics during baseball pitching

R. Tyler Richardson

School of Behavioral Sciences and Education, Pennsylvania State University Harrisburg, 777 W. Harrisburg Pike, Middletown, PA 17057, USA

ARTICLE INFO

Article history:
Accepted 25 November 2020

Keywords:
Scapula
Shoulder
Pitching
Kinematics
Biomechanics

ABSTRACT

Assessment of scapulothoracic and glenohumeral contributions to shoulder function during baseball pitching are limited by challenges in accurately measuring dynamic scapular orientation. A recently validated individualized linear model approach that estimates scapular orientation based on measurable humerothoracic orientation has yet to be adapted for pitching and may improve upon currently recommended methods such as the acromion marker cluster (AMC). This study evaluates the ability of a pitching-specific individualized linear model to estimate scapular orientation in static positions throughout a throwing motion by comparing against palpation and an AMC. Individualized linear models were created for 14 collegiate pitchers by determining scapulothoracic and humerothoracic orientations at static arm postures throughout their individual dynamic throwing motions. Linear model and AMC estimates were compared against palpation at intermediate test positions within the throwing motion that were excluded from model creation. Linear model estimates were similar to palpation at all test positions and on all scapulothoracic axes while AMC estimates differed on internal/external rotation and anterior/posterior tilt during cocking (p = 0.001, p = 0.018) and follow-through (p = 0.003, p = 0.006). Linear model root mean square error (RMSE) values were smaller than AMC values for all positions/axes. Linear model RMSE values (2.8–6.3°) were within a range of published values previously deemed acceptable, while AMC values (5.1–15.8°) went beyond this range. The linear model approach accurately estimates static scapular orientation throughout a pitching motion and improves upon current methods. Future applications to dynamic pitching may facilitate understanding of how scapulothoracic and glenohumeral joint function relate to injury risks, rehabilitation, and performance.

1. Introduction

Baseball pitching regularly results in injury with incidence rates ranging from 1.89 to 4.16 injuries per athlete-game exposures (Collins and Comstock, 2008; Posner et al., 2011). The shoulder is the most injured site in the body representing 30.7–34.2% of all pitching injuries (Collins and Comstock, 2008; Posner et al., 2011). Majority of shoulder injuries primarily involve the glenohumeral joint (Braun et al., 2009; Wilk et al., 2009) and are associated with long recovery times (Collins and Comstock, 2008; Wilk et al., 2009; Zaremski and Krabak, 2012), recurring injury (Krajnik et al., 2010; Powell and Barber-Foss, 2000), and decreased performance or failure to return to sport (Harris et al., 2013; Mazoue and Andrews, 2006). The repetitive bouts of high loading and rapid rotational motion at the shoulder during pitching (Dillman et al., 1993; Dun et al., 2008) indicate that mechanics play a crucial role in injury risk (Chalmers et al., 2017). Accordingly, knowledge of glenohumeral joint mechanics is essential to understanding factors related to performance and injury associated with pitching.

Nearly all biomechanical analyses of pitching only examine humerothoracic kinematics (Thompson et al., 2018). Studies that have investigated scapulothoracic and/or glenohumeral function are either limited to static analysis and/or examine non-throwing motions (Kibler et al., 2012; McHugh et al., 2016; Myers, 2005; Park et al., 2020; Pellegrini et al., 2013; Seitz et al., 2012), evaluate a throwing motion at slow speeds (Meyer et al., 2008; Saka et al., 2015), and/or utilize scapular tracking methods that have not been specifically validated for estimating scapular motion during an overhead throwing motion (Holt and Oliver, 2016; Konda et al., 2015; Nissen et al., 2007; Okamoto et al., 2018; Oliver et al., 2019). Traditional, skin-based motion capture can measure 3-dimensional (3D) orientations of upper extremity segments but fails to track the scapula due to its independent motion beneath the skin (Karduna et al., 2001; van Andel et al., 2009). Without accurate measures of scapular motion, glenohumeral and scapu-

E-mail address: rtr12@psu.edu

https://doi.org/10.1016/j.jbiomech.2020.110160
0021-9290/

lothoracic contributions to global shoulder motion cannot be determined.

The acromion marker cluster (AMC) (van Andel et al., 2009) is the currently recommended method to estimate dynamic scapular orientation (Lempereur et al., 2014). The AMC produces acceptable errors during activities of daily living (Lempereur et al., 2014), but may be unsuitable for pitching due to its reduced accuracy at humerothoracic elevations above 90° (Brochard et al., 2011; Lempereur et al., 2014; van Andel et al., 2009) and during rotational arm motions (Chu et al., 2012), and susceptibility to soft tissue artifact (Lempereur et al., 2014; Meskers et al., 2007; Shaheen et al., 2011; van Andel et al., 2009).

A new linear model approach has been recently validated to measure scapular kinematics (Nicholson et al., 2017). This method develops individualized linear model equations to estimate dynamic scapular orientation based on measurable humerothoracic orientations and acromion process locations derived from a set of static calibration positions. This approach performs accurately at all levels of humerothoracic elevation and for rotational arm motions (Nicholson et al., 2017), but has yet to be adapted and evaluated for baseball pitching.

The objective of this study was to develop a pitching-specific individualized linear model and assess its ability to estimate scapulothoracic orientation in static positions throughout a throwing motion by comparing it to palpation and against the AMC. It was hypothesized that linear model estimates would be similar to palpation while AMC estimates would be different. It was also hypothesized linear model root mean square errors (RMSE) would be within a range of published values previously deemed acceptable (Lempereur et al., 2014) while the AMC would be beyond this range.

2. Methods

2.1. Subjects

Fourteen male Division III collegiate baseball pitchers (18–22 years) participated. Informed consent was obtained in accordance with the University's human subjects review board. All subjects were healthy at the time of testing and were full participants in practice and games.

2.2. Dynamic throwing

Subjects completed a self-directed warm up. Retroreflective markers were placed on the trunk (sternum, T1/T8 spinous processes), humerus (medial/lateral epicondyles, posterolateral humerus), forearm (radial/ulnar styloid processes, distal radius), and hand (dorsum of 2nd and 4th metacarpals) segments. An AMC was adhered to the acromion process with the triad's central marker positioned directly over the landmark. Subjects threw from flat ground and were instructed to aim for a target region marked on a net positioned 8 m away and to throw as hard as they felt comfortable while maintaining accuracy. Each subject completed six fastball trials. A ten-camera motion capture system (Qualisys, Gothenburg, Sweden) collecting at 240 Hz recorded all 3D motion data while ball velocity was measured with a radar sensor (TriGreat USA Corp., Gardena, CA).

2.3. Calculation of static calibration and test positions

Only each subject's fastball trial with the greatest ball velocity was used to develop their individualized linear model as it was presumed to possess the largest range of humerothoracic motion. Segment coordinate systems were constructed (Wu et al., 2005) and Euler YZY humerothoracic kinematics were calculated. Each trial was trimmed to begin at maximum humerothoracic horizontal abduction during early cocking and end at maximum humerothoracic horizontal adduction during follow-through. Six events representing the extremes of shoulder motion occurring during the throwing motion of each subject's fastball trial were identified: 1/2) maximum/minimum humerothoracic horizontal abduction, 3/4) maximum/minimum humerothoracic elevation, 5/6) maximum/minimum humeral external rotation (Fig. 1). Humerothoracic orientations at these events served as static calibration positions to develop each subject's individualized linear model with the exception of the maximum horizontal abduction and maximum humeral external rotation postures. Subjects were unable to reproduce the extreme arm postures at these two events in a static scenario. Alternatively, subjects were asked to recreate more achievable arm postures occurring at 75% of maximum humerothoracic horizontal abduction and 75% of maximum humeral external rotation during the pitch (Fig. 1). These alternative arm postures replaced the corresponding original extreme postures to serve as static calibration positions for linear model creation. Finally, three intermediate static test positions were identified to test the accuracy of the linear model and AMC. Humerothoracic orientations at these test positions were determined as arm postures at: 1) cocking phase - mid-point on humerothoracic Y″ between 75% of maximum humerothoracic horizontal abduction and maximum humeral external rotation, 2) acceleration phase - mid-point on humerothoracic Y″ between 75% of maximum humeral external rotation and maximum humeral internal rotation, and 3) follow-through phase - mid-point in time between maximum humeral internal rotation and maximum humerothoracic horizontal adduction (Fig. 1).

2.4. Static position matching

Real-time feedback with motion capture was employed to recreate humerothoracic orientations at each static position. An interactive animation including an avatar with two arms – target arm and real-time arm – was displayed (Fig. 2). The target arm was positioned in the humerothoracic orientation of one of the static positions while the real-time arm followed the humerothoracic orientation of the subject's arm as it moved in real-time. For each calibration and test position, subjects were instructed to match the

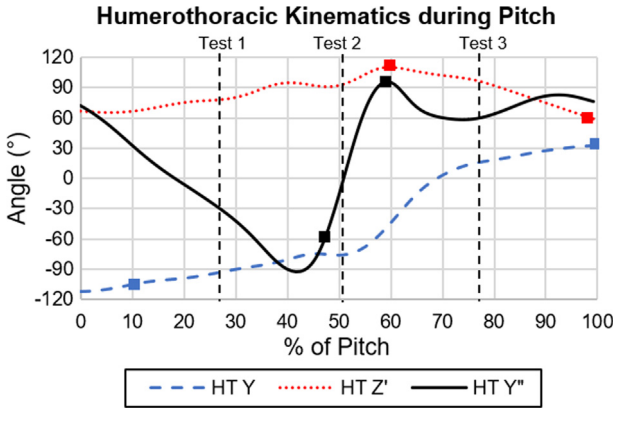

Fig. 1. Humerothoracic kinematics during a pitch trial from maximum horizontal abduction (0% of pitch) to maximum horizontal adduction (100% of pitch) for a representative subject. Angles calculated using an Euler YZY sequence where HT Y = horizontal adduction (+)/abduction (-), HT Z' = elevation (+)/depression (-), and HT Y″ = humeral internal (+)/external (-) rotation. Six key events used to determine arm postures for static calibration positions identified as extreme points on each degree of freedom are displayed with squares. Events for intermediate static test positions shown as dashed vertical lines.

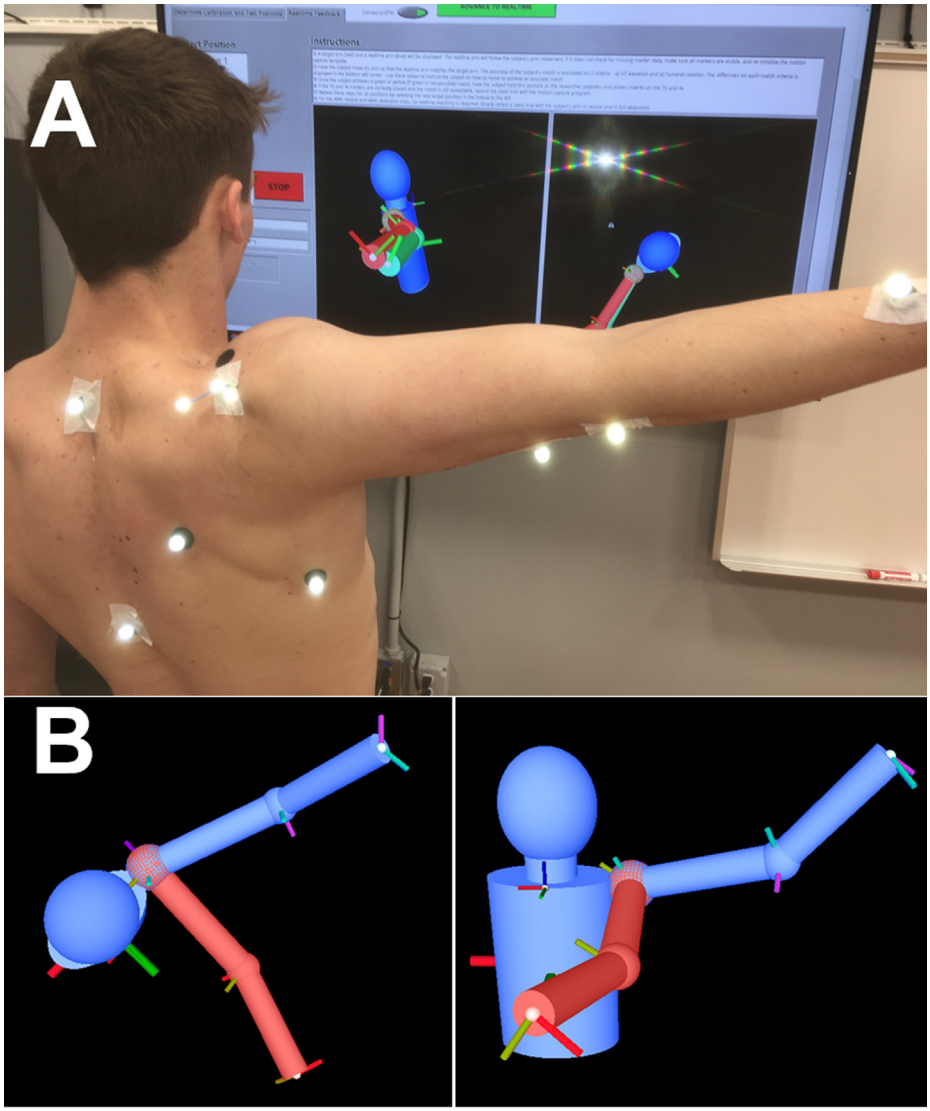

Fig. 2. (A) Subject wearing static marker set during static position match using real-time feedback with motion capture. Scapular markers (trigonum spinae and inferior angle) were re-positioned for each static matching trial. (B) Two views of the real-time visual feedback avatar displayed to the subject to facilitate accurate position matching. Target arm (red) and real-time matching arm controlled by the subject's movements (blue) are shown. (For interpretation of the references to color in this figure legend, the reader is referred to the web version of this article.)

real-time arm to the target arm. The difference in 3D humerothoracic orientation between the real-time and target arms was calculated in real-time using a helical approach (Woltring et al., 1985). The color of the real-time arm would change from blue to yellow indicating an acceptable match (10–20° difference in 3D orientation) or to green indicating an ideal match (<10° difference in 3D orientation). All subjects attempted to achieve an ideal match; however, an acceptable match was utilized if this was not possible. The 3D humerothoracic match thresholds were based on pilot testing and correspond to a 2–3° difference on each of the three 1D humerothoracic axes – similar to the accuracy associated with palpation (de Groot, 1997). Once matched, subjects maintained the desired position while scapular markers (trigonum spinae and inferior angle) were placed and upper extremity orientation was recorded. This process was repeated for each additional static position. Finally, two more static positions – 1) arm resting at side and 2) arm fully abducted in the coronal plane – were collected for the double calibration AMC method (Brochard et al., 2011). For both positions, scapular markers were placed and upper extremity orientation was recorded.

2.5. Calculation of joint angles

Trunk and humerus coordinate systems were constructed based on ISB recommendations (Wu et al., 2005), while the scapular coordinate system used the acromion process marker in place of an acromial angle marker (Nicholson et al., 2017; Rapp et al., 2017; Richardson et al., 2016). Humerothoracic angles were calculated using an Euler YZY sequence due to the presence of discontinuities when using the recommended Euler YXY sequence (Wu et al., 2005). Scapulothoracic joint angles were calculated using an Euler YXZ sequence (Wu et al., 2005).

2.6. Individualized linear model creation and AMC calibration

Individualized linear model equations were created based on the static calibration position data (Nicholson et al., 2017) with one equation for each of scapulothoracic axis of motion. Each equation utilized measurable humerothoracic YZY angles as predictor variables. The equations were then applied to provide estimates of 3D scapulothoracic orientation based on the measured

humerothoracic orientation recorded during static test positions. AMC estimates of scapular orientation were determined using the double calibration method (Brochard et al., 2011).

2.7. Evaluation of accuracy

Linear model and AMC estimates of scapulothoracic orientation were compared against a palpation reference standard in each test position. RMSE values were calculated between each method and palpation at each position and on each scapulothoracic axis of motion. A three-way repeated measures analysis of variance (ANOVA) with factors of 1) method (palpation, linear model, AMC), 2) test position (cocking, acceleration, follow-through), and 3) axis of scapulothoracic motion (upward/downward rotation, internal/external rotation, anterior/posterior tilt) was conducted. Pending a significant interaction, post hoc analyses examined scapulothoracic angle estimates between each method at each position along each scapulothoracic axis. Alpha level was set at $\alpha = 0.05$. Bonferroni corrections were applied to account for multiple pairwise comparisons. Statistical analyses were performed in SPSS (SPSS v26, IBM, Armonk, NY).

3. Results

All subjects achieved at least an acceptable (<20°) 3D humerothoracic match for all static positions.

The linear model generated smaller RMSE values than the AMC on all scapular axes for each test position (Fig. 3). The ANOVA did

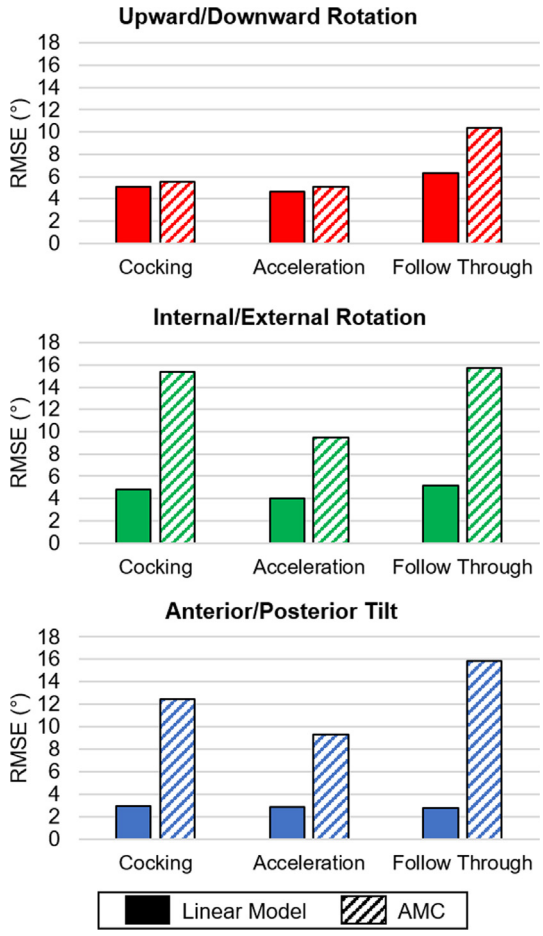

Fig. 3. Root mean square errors for the linear model and AMC at each static test position.

Table 1
Results of the post hoc testing on each scapulothoracic axis comparing each method (linear model and AMC) to palpation at each static test position.

Test Position	Parameter	Upward (+)/Downward (-) Rotation			Internal (+)/External (-) Rotation			Posterior (+)/Anterior (-) Tilt		
		Palp.	Linear Model	AMC	Palp.	Linear Model	AMC	Palp.	Linear Model	AMC
1 – Cocking	Angle 95% CI (°)	31.3–36.5	29.7–37.5	28.9–36.1	15.8–25.0	17.7–27.6	2.0–11.7	6.5–10.8	5.1–10.6	12.1–23.4
	Mean Diff. (95% CI) (°)		−0.3 (−4.3–3.5)	−1.4 (−5.5–2.6)		2.2 (−1.0–5.5)	**−13.6 (−19.0–8.1)**		−0.7 (−2.9–1.5)	**9.1 (2.6–15.6)**
	p-value		1.000	1.000		0.726	**<0.001**		1.000	**0.018**
2 – Acceleration	Angle 95% CI (°)	29.1–36.7	31.6–37.0	31.3–36.1	26.6–35.8	25.7–34.0	21.6–31.3	−0.5–4.2	−0.3–4.8	−1.7–10.5
	Mean Diff. (95% CI) (°)		1.6 (−1.7–4.9)	0.9 (−2.9–4.7)		−1.4 (−4.2–1.5)	−4.8 (−11.0–1.4)		0.4 (−1.8–2.5)	2.5 (−4.3–9.4)
	p-value		1.000	1.000		1.000	0.489		1.000	1.000
3 – Follow-Through	Angle 95% CI (°)	24.8–37.6	22.3–35.2	28.0–37.6	52.6–62.9	51.5–60.5	63.4–76.8	−11.5–5.9	−9.0 –4.8	−27.0–15.0
	Mean Diff. (95% CI) (°)		−2.4 (−6.9–2.0)	1.7 (−6.1–9.4)		−1.8 (−5.5–1.8)	**12.3 (5.0–19.7)**		1.7 (0.1–3.4)	**−12.3 (−19.9–4.8)**
	p-value		1.000	1.000		1.000	**0.003**		0.123	**0.006**

95% confidence intervals (CI) for scapular orientations and differences between each method and palpation are shown. Mean differences displayed as (Linear Model – Palpation) or (AMC – Palpation). Significant differences (Bonferroni adjusted *p*-values < 0.05) are bolded.

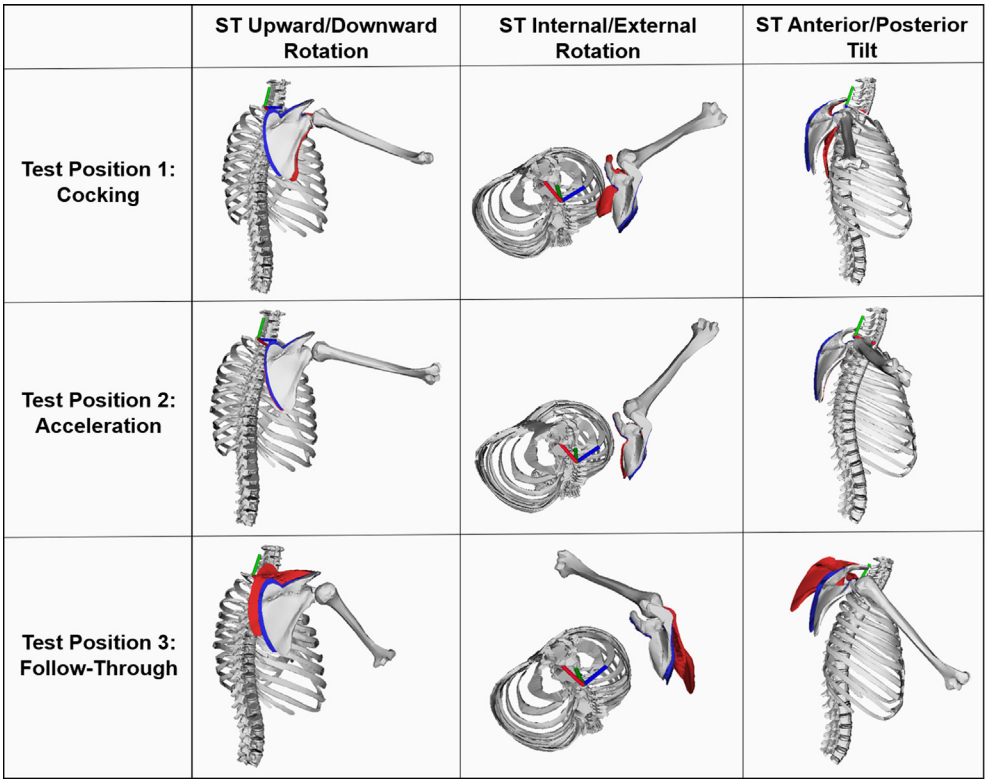

Fig. 4. Skeletal models displaying scapular orientations determined from palpation (white) and estimated by the linear model (blue) and AMC (red) on each scapular axis of motion and at each static test position from a representative subject. (For interpretation of the references to color in this figure legend, the reader is referred to the web version of this article.)

not reveal a significant difference for the main effect of measurement method ($F_{2,26}$ = 1.095, p = 0.350). However, significant interaction effects between measurement method and position ($F_{4,24}$ = 6.466, p = 0.005) and measurement method, position, and axis ($F_{8,20}$ = 32.057, p < 0.001) indicated that differences were present between approaches. Post hoc testing along each scapulothoracic axis revealed several cases where methods differed from palpation (Table 1). No significant differences existed between the linear model and palpation. The AMC was similar to palpation on upward/downward rotation, however differences were found on internal/external rotation and anterior/posterior tilt at the cocking (mean difference = 13.6°, p < 0.001; mean difference = −9.1°, p = 0.018) and follow-through test positions (mean difference = −12.4°, p = 0.003; mean difference = −12.3°, p = 0.006). Skeletal models of a representative subject are displayed in Fig. 4 to illustrate differences between each method and palpation.

4. Discussion

Linear model estimates of scapular orientation were similar to those determined by palpation on all scapular axes of motion for every test position. These results largely agree with published, non-pitching linear model evaluations (Nicholson et al., 2017; Rapp et al., 2017). AMC estimates were similar to palpation on upward/downward rotation but were significantly different on internal/external rotation and anterior/posterior tilt in the cocking and follow-through positions. These results predominantly agree with similar previous AMC evaluations (Karduna et al., 2001; Rapp et al., 2017). The cocking and follow-through positions often involve considerable soft tissue deformation over the acromion from the deltoid. The AMC's large average errors coupled with its fluctuations between over- and under-estimation on both internal/external rotation and anterior/posterior tilt potentially indicate that soft tissue deformation may underlie these errors as other studies have suggested (Karduna et al., 2001; van Andel et al., 2009). Collectively, these results confirm the hypotheses that linear model estimates are similar to palpation while AMC estimates are different than palpation.

A systematic review of marker-based methods for measuring scapular motion reported a range of RMSE values for upward/-downward rotation (1.6–14.2°), internal/external rotation (1.6–11.4°), and anterior/posterior tilt (1.4–10.3°) (Lempereur et al., 2014). In the present study, linear model's RMSE values were well within these ranges while AMC's RMSE values were beyond published values on internal/external rotation and anterior/posterior tilt. These results confirm the hypotheses that linear model RMSE values are within a range of published values while AMC values are beyond this range. Linear model RMSE values about each axis were similar across all test positions indicating consistent accuracy throughout a throwing motion. AMC errors for the cocking and follow-through positions were notably larger than those for the acceleration position. The abduction arm posture used in the AMC double calibration process (Brochard et al., 2011) was most similar to the arm configuration of the acceleration test position which may explain the improved AMC accuracy at this position. These findings are also consistent with known limitations of the AMC for arm configurations involving significant humeral rotation (Chu et al., 2012) and show that this method is not consistently accurate throughout a pitching motion.

There are several limitations to this study. Pitchers threw from flat ground at less than a standard pitching distance. Palpation was used as a reference standard for evaluation. While not a gold standard, palpation is capable of measuring scapular orientation within 2° (de Groot, 1997) and was utilized in similar studies (Lempereur

et al., 2014; Rapp et al., 2017). The linear model approach makes two key assumptions. First, it assumes that scapular orientation at a given humerothoracic orientation is identical for both static and dynamic scenarios. Muscle forces influencing scapular orientation likely differ between static and dynamic scenarios, however, literature has reported that scapular orientation is similar between loaded and unloaded conditions (de Groot et al., 1999). Regardless, researchers should be cognizant of this assumption if using the linear model to estimate scapular orientations in a dynamic pitching scenario. Second, linear model estimates depend on humerothoracic orientations and are susceptible to errors when dynamic humerothoracic inputs go beyond static humerothoracic input bounds used to create the model. These "out-of-bounds" errors are most likely to occur around maximum humeral external rotation where subjects were unable to recreate full dynamic external rotation in a static scenario. Consequently, caution should be exercised when interpreting linear model estimates near dynamic maximum shoulder external rotation. Future evaluation of the linear model under dynamic conditions is warranted to better understand the ability of this approach to estimate scapular orientation at maximum external rotation during a pitch.

5. Conclusion

This static analysis represents the most comprehensive validation of a non-invasive method for estimating scapular orientation during pitching. The individualized linear model approach accurately estimates static scapular orientations throughout a full speed pitching motion and improves upon current methods. While validation in a dynamic setting remains a substantial challenge, these findings suggest that the linear model may be a viable approach for accurately estimating scapulothoracic and glenohumeral kinematics throughout a full speed pitch. Future applications to dynamic pitching may provide previously unknown joint-specific information to facilitate understanding of how scapulothoracic and glenohumeral function relate to injury risks, rehabilitation, and performance.

Declaration of Competing Interest

The authors declare that they have no known competing financial interests or personal relationships that could have appeared to influence the work reported in this paper.

Acknowledgements

The author would like to thank Alyssa Knisley, Brandon Hoover, and Jesse Donahue for their assistance with data collection.

References

Braun, B.S., Kokmeyer, D., Millett, P.J., 2009. Shoulder Injuries in the Throwing Athlete. J. Bone Jt. Surg. 91, 966–978.
Brochard, S., Lempereur, M., Rémy-Néris, O., 2011. Double calibration: an accurate, reliable and easy-to-use method for 3D scapular motion analysis. J. Biomech. 44, 751–754.
Chalmers, P.N., Wimmer, M.A., Verma, N.N., Cole, B.J., Romeo, A.A., Cvetanovich, G.L., Pearl, M.L., 2017. The Relationship Between Pitching Mechanics and Injury: A Review of Current Concepts. Sports Health 9, 216–221.
Chu, Y., Akins, J., Lovalekar, M., Tashman, S., Lephart, S., Sell, T., 2012. Validation of a video-based motion analysis technique in 3-D dynamic scapular kinematic measurements. J. Biomech. 45, 2462–2466.
Collins, C.C.L., Comstock, R.D., 2008. Epidemiological features of high school baseball injuries in the United States, 2005–2007. Pediatrics 121, 1181–1187.
de Groot, J.H., 1997. The variability of shoulder motions recorded by means of palpation. Clin. Biomech. 12, 461–472.
de Groot, J.H., Van Woensel, W., Van Der Helm, F.C., 1999. Effect of different arm loads on the position of the scapula in abduction postures. Clin. Biomech. 14, 309–314.
Dillman, C., Fleisig, G., Andrews, J., 1993. Biomechanics of Pitching with Emphasis upon Shoulder Kinematics. J. Orthop. Sport. Phys. Ther. 18, 402–408.
Dun, S., Loftice, J., Fleisig, G.S., Kingsley, D., Andrews, J.R., 2008. A biomechanical comparison of youth baseball pitches: Is the curveball potentially harmful?. Am. J. Sports Med. 36, 686–692.
Harris, J.D., Frank, J.M., Jordan, M.A., Bush-Joseph, C.A., Romeo, A.A., Gupta, A.K., Abrams, G.D., McCormick, F.M., Bach, B.R., 2013. Return to sport following shoulder surgery in the elite pitcher: a systematic review. Sports Health 5, 367–376.
Holt, T., Oliver, G.D., 2016. Hip and upper extremity kinematics in youth baseball pitchers Hip and upper extremity kinematics in youth baseball pitchers. J. Sports Sci. 34, 856–861.
Karduna, A.R., McClure, P.W., Michener, L.A., Sennett, B., 2001. Dynamic measurements of three-dimensional scapular kinematics: a validation study. J. Biomech. Eng. 123, 184–190.
Kibler, W.B., Sciascia, A., Moore, S., 2012. An acute throwing episode decreases shoulder internal rotation. Clin. Orthop. Relat. Res. 470, 1545–1551.
Konda, S., Yanai, T., Sakurai, S., 2015. Configuration of the shoulder complex during the arm-cocking phase in baseball pitching. Am. J. Sports Med. 43, 2445–2451.
Krajnik, S., Fogarty, K.J., Yard, E.E., Comstock, R.D., 2010. Shoulder injuries in US High School Baseball and Softball Athletes, 2005–2008. Pediatrics 125, 497–501.
Lempereur, M., Brochard, S., Leboeuf, F., Rémy-Néris, O., 2014. Validity and reliability of 3D marker based scapular motion analysis: a systematic review. J. Biomech. 47, 2219–2230.
Mazoue, C., Andrews, J., 2006. Repair of full-thickness rotator cuff tears in profesional baseball players. Am. J. Sports Med. 34, 182189.
McHugh, M.P., Tyler, T.F., Mullaney, M.J., Mirabella, M.R., Nicholas, S.J., 2016. The effect of a high pitch volume on musculoskeletal adaptations in high school baseball pitchers. Am. J. Sports Med. 44, 2246–2254.
Meskers, C.G.M., van de Sande, M.A.J., de Groot, J.H., 2007. Comparison between tripod and skin-fixed recording of scapular motion. J. Biomech. 40, 941–946.
Meyer, K.E., Saether, E.E., Soiney, E.K., Shebeck, M.S., Paddock, K.L., Ludewig, P.M., 2008. Three-dimensional scapular kinematics during the throwing motion. J. Appl. Biomech. 24, 24–34.
Myers, J.B., 2005. Scapular position and orientation in throwing athletes. Am. J. Sports Med. 33, 263–271.
Nicholson, K.F., Richardson, R.T., Rapp, E.A., Quinton, R.G., Anzilotti, K.F., Richards, J. G., 2017. Validation of a mathematical approach to estimate dynamic scapular orientation. J. Biomech. 54, 101–105.
Nissen, C.W., Westwell, M., Õunpuu, S., Patel, M., Tate, J.P., Pierz, K., Burns, J.P., Bicos, J., 2007. Adolescent baseball pitching technique: a detailed three-dimensional biomechanical analysis. Med. Sci. Sports Exerc. 39, 1347–1357.
Okamoto, S., Endo, Y., Saito, R., Nakazawa, R., Sakamoto, M., 2018. Three-dimensional kinematic analysis of glenohumeral, scapular, and thoracic angles at maximum shoulder external rotation associated with baseball shadow pitching: comparison with normal pitching. J. Phys. Ther. Sci. 30, 938–942.
Oliver, G.D., Plummer, H., Henning, L., Saper, M., Glimer, G., Brambeck, A., Andrews, J.R., 2019. Effects of a simulated game on upper extremity pitching mechanics and muscle activations among various pitch types in youth baseball pitchers. J. Pediatr. Orthop. 39, 387–393.
Park, J., Kim, J., Seo, B.H., Yu, H.D., Sim, J.H., Lee, J.H., 2020. Three-dimensional analysis of scapular kinematics during arm elevation in baseball players with scapular dyskinesis: comparison of dominant and nondominant arms. J. Sport Rehabil. 29, 93–101.
Pellegrini, A., Tonino, P., Paladini, P., Cutti, A., Ceccarelli, F., Porcellini, G., 2013. Motion analysis assessment of alterations in the scapulo-humeral rhythm after throwing in baseball pitchers. Musculoskelet. Surg. 97, S9–S13.
Posner, M., Cameron, K.L., Wolf, J.M., Belmont, P.J., Owens, B.D., 2011. Epidemiology of major league baseball injuries. Am. J. Sports Med. 39, 1676–1680.
Powell, J.W., Barber-Foss, K.D., 2000. Sex-related injury patterns among selected high school sports. Am. J. Sports Med. 28, 385–391.
Rapp, E.A., Richardson, R.T., Russo, S.A., Rose, W.C., Richards, J.G., 2017. A comparison of two non-invasive methods for measuring scapular orientation in functional positions. J. Biomech. 61, 269–274.
Richardson, R.T., Nicholson, K.F., Rapp, E.A., Johnston, T.E., Richards, J.G., 2016. A comparison of acromion marker cluster calibration methods for estimating scapular kinematics during upper extremity ergometry. J. Biomech. 49, 1255–1258.
Saka, M., Yamauchi, H., Yoshioka, T., Hamada, H., Gamada, K., 2015. Scapular kinematics during late cocking of a simulated throwing activity in baseball players with shoulder injury: a cross-sectional study using a 3D-to-2D registration technique. J. Sport Rehabil. 24, 91–98.
Seitz, A.L., Reinold, M., Schneider, R.A., Gill, T.J., Thigpen, C.A., 2012. No effect of scapular position on 3-dimensional scapular motion in the throwing shoulder of healthy professional pitchers. J. Sport Rehabil. 21, 186–193.
Shaheen, A., Alexander, C., Bull, A., 2011. Effects of attachment position and shoulder orientation during calibration on the accuracy of the acromial tracker. J. Biomech. 44, 1410–1413.
Thompson, S.F., Guess, T.M., Plackis, A.C., Sherman, S.L., Gray, A.D., 2018. Youth baseball pitching mechanics: a systematic review. Sports Health 10, 133–140.
van Andel, C., van Hutten, K., Eversdijk, M., Veeger, D., Harlaar, J., 2009. Recording scapular motion using an acromion marker cluster. Gait Posture 29, 123–128.
Wilk, K.E., Obma, P., Simpson, C.D., Cain, E.L., Dugas, J.R., Andrews, J.R., 2009. Shoulder injuries in the overhead athlete. J. Orthop. Sports Phys. Ther. 39, 38–54.

Woltring, H.J., Huiskes, R., de Lange, A., Veldpaus, F.E., 1985. Finite centroid and helical axis estimation from noisy landmark measurements in the study of human joint kinematics. J. Biomech. 18, 379–389.
Wu, G., Van Der Helm, F.C.T., Veeger, H.E.J., Makhsous, M., Van Roy, P., Anglin, C., Nagels, J., Karduna, A.R., McQuade, K., Wang, X., Werner, F.W., Buchholz, B., 2005. ISB recommendation on definitions of joint coordinate systems of various joints for the reporting of human joint motion - Part II: Shoulder, elbow, wrist and hand. J. Biomech. 38, 981–992.
Zaremski, J.L., Krabak, B.J., 2012. Shoulder injuries in the skeletally immature baseball pitcher and recommendations for the prevention of injury. Phys. Med. Rehabil. 4, 509–516.